Laser generation thresholds of the cholesteric liquid crystal layer

A.A. Malinchenko[1], *N.A. Vanyushkin*[2], *A.V. Bulanov*[3], *A.H. Gevorgyan*[1,3]
[1] *Far Eastern Federal University, Institute of High Technologies and Advanced Materials, 10 Ajax Bay, Russky Island, Vladivostok, 590922, Russia;*
[2] *Moscow Institute of Physics and Technology, Phystech School of Electronics, Photonics and Molecular Physics, Institutsky lane 9, Dolgoprudny, 141700, Russia;*
[3] *V.I. Il'ichev Pacific Oceanological Institute Far Eastern Branch of the Russian Academy of Science, 43 Bal – 43 Baltiyskaya Str, Vladivostok, 690041, Russia*

Abstract

The laser threshold of the eigenmodes in cholesteric liquid crystal (CLC) cells are calculated. The influence of gain on light localization was investigated. The influence of absorption and gain on the light energy density in the CLC layer both at isotropic and anisotropic absorption and gain were investigated for the first time. The calculated threshold values were compared with analytical expression for laser thresholds obtained under the condition ImK<<1/d, where d is the CLC layer thickness, and K is the resonance wave vector.

Keywords: cholesteric liquid crystal, laser threshold, eigenmodes, gain, absorption.

Citation: Malinchenko AA, Vanyushkin NA, Bulanov AV, Gevorgyan AH. Laser generation thresholds of the cholesteric liquid crystal layer. Computer Optics 2025; 49(6): 916-923. DOI: 10.18287/2412-6179-CO-1643.

Introduction

The study of the peculiarities of laser generation by a layer of cholesteric liquid crystal (CLC) is of both great theoretical interest and large practical application. The idea of laser generation in media with spatially periodic media was formulated by Kogelnik and Shank [1] and was later treated in many papers (see [2] and references therein). Dowling and colleagues [3] reported that, with the inclusion of a fluorescent emitter, spontaneous emission would be suppressed within a photonic band gap (PBG) and enhanced at the band edges where there is a sharp increase in the photonic density of states (PDS). It is here at the PBG borders that lasing occurs on the inclusion of such a gain medium, as first for CLC reported in [4, 5]. Let us note that firstly in 1981, Il'chishin and coworkers [6] demonstrated the modification of fluorescent emission in the presence of a PBG in CLC. Implementation of the Kogelnik and Shank idea in cholesteric and nematic liquid crystals has stimulated researcher interest in photonic crystal physics and has led to the creation of liquid crystalline lasers [7, 8]. In [9] proposed a model for laser generation in CLC's that makes use of kinetic equations for the excited states populations and generated light. Since 2000, a rapid theoretical and experimental study of the peculiarities of laser generation in a variety of different liquid-crystal structures and phases: in CLC phase, in the chiral smectic phase, in polymeric liquid-crystals, in cholesteric elastomers, in solid cholesterics, in an intermediate phase between the chiral nematic phase and the smectic A phase, and in blue phases I and II, and in LC-containing structures, including CLC with defect in its structure, and also random lasing in CLC, were widely investigated. In addition, the tuning of the band edge lasing under the influence of external stimuli such as temperature, ultraviolet illumination, mechanical stress and external electric, magnetic and light fields have also been widely investigated (see Ref. [10 – 28] and the literature cited therein). The CLC layer gives rise to a polarization-sensitive laser generation. The main advantages of CLC lasers are their small size, simplicity of fabrication, possibility of mirrorless generation, possibility of smooth control of laser generation wavelength in a wide range, possibility of multifrequency laser generation, etc.

In this paper for the first time, we investigated the lasing threshold peculiarities of the dye dopped CLC layer at isotropic and anisotropic gain, its dependence on CLC layer thickness and edge mode numbers.

1. Models and methodology

Let us consider light propagation through a planar CLC layer (Fig. 1). CLCs have a self-organized helical structure (it can be regarded as a 1D photonic crystal), the periodic structure of which gives rise to a polarization-sensitive photonic band gap (PBG) in the wavelength band $pn_o < \lambda < pn_e$, where n_o and n_e are the ordinary and extraordinary local refractive indices of CLC. Within PBG only the circularly polarized light having the same handedness as the CLC helix itself is selectively reflected (at normal light incidence) while transmitting light with opposite handedness.

The tensors of dielectric permittivity and magnetic permeability of CLCs in the laboratory coordinate frame have the forms:

$$\hat{\varepsilon}(z) = \varepsilon_m \begin{pmatrix} 1+\delta\cos 2az & \pm\delta\sin 2az & 0 \\ \pm\delta\sin 2az & 1-\delta\cos 2az & 0 \\ 0 & 0 & 1-\delta \end{pmatrix}, \quad (1)$$
$$\hat{\mu}(z) = \hat{I},$$

where $\varepsilon_m = (\varepsilon_1 + \varepsilon_2)/2$, $\delta = (\varepsilon_1 - \varepsilon_2)/(\varepsilon_1 + \varepsilon_2)$, $\varepsilon_{1,2} = n_{e,o}^2$ are the principal values of the local dielectric permittivity tensor, $a = 2\pi/p$, p is the pitch of the helix.

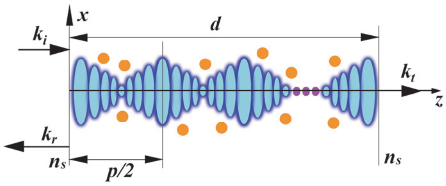

Fig. 1. The geometry of the problem. The large ellipsoids represent the anisotropic molecules, which are rotating continuously forming a helicoidal structure along the z-axis. p is the helix pitch, that is the spatial period of the structure, d is CLCs layer thickness, $\boldsymbol{k_i}$, $\boldsymbol{k_r}$ and $\boldsymbol{k_t}$ are the wave vectors of the incident, reflected and transmitted waves respectively, the orange spheres represent the dye molecules. The CLC layer on its both sides borders with isotropic half-spaces with the same refractive indices equal to n_s

The exact analytical solution of Maxwell's equations for CLCs is known (see [29, 30]) and the dispersion equation has the form [30]:

$$\left(\frac{\omega^2}{c^2}\varepsilon_1 - K_m^2 - a^2\right)\times \left(\frac{\omega^2}{c^2}\varepsilon_2 - K_m^2 - a^2\right) - 4a^2K_m^2 = 0, \quad (2)$$

where K_m are the z components of wave vectors $(m = 1,2,3,4)$, ω is the cyclic frequency and c is the velocity of light in vacuum.

Using exact analytical solution of the Maxwell's equations, and dispersion equation (2) we can solve the problem of light reflection, transmission, and absorption or amplification in the case of a planar CLC layer of finite thickness. We assume that the optical axis of the CLC layer is perpendicular to the boundaries of the layer and is directed along the z-axis. The CLC layer on its both sides borders isotropic half-spaces with the same refractive indices equal to n_s. The boundary conditions, consisting of the continuity of the tangential components of the electric and magnetic fields, are a system of eight linear equations with eight unknowns. Let us note that the analytical solution of this boundary-value problem is also known [31]. By solving this boundary-value problem, one can determine the values of the reflected $\mathbf{E}_r$ and transmitted $\mathbf{E}_t$ fields and calculate the total field in the CLC layer in every z point $\mathbf{E}_{in}(z)$, and etc.

2. Results and discussion

Below, the ordinary and extraordinary refractive indices of the CLC layers are taken to be $n_o = \sqrt{\varepsilon_2} = 1.4639$ and $n_e = \sqrt{\varepsilon_1} = 1.5133$, the CLC layer helix is right-handed, and its pitch is: $p = 420$ nm, CLC layer thickness is: d=50p. We will consider the light normal incidence case and the case of minimal influence of dielectric boundaries, that is the case $n_s = \sqrt{\varepsilon_m}$. So, the light with right circular polarization incident on the CLC has a PBG which at these parameters of CLC layer is in the range about [615 ÷ 635] nm, but the light with left circular polarization does not. We investigate the peculiarities of the threshold for the eigenmodes. The eigenmodes have polarizations coincidence with eigenpolarizations (EPs). By definition, the EPs are the two polarizations of incident light that do not change as the light passes through the system. One of the EPs approximately coincides with the right circular polarization (we will call it the diffracting EP) and the other one with the left circular polarization (the non-diffracting EP).

Now about PDS. The PDS is usually understood as the "number of states" with different wave vectors k in a unit spectral interval dω, which can be represented as $\rho = dk/d\omega$. There exist several ways to calculate PDS which are described and compared in detail [32]. In many cases it is convenient to calculate it via so called phase time (or Wigner time) τ_φ which requires only spectral dependence of transmission coefficient t:

$$\rho_m = -\frac{\lambda^2}{2\pi c d}\frac{d}{d\lambda}\mathrm{Arg}(t_{1,2}) = -\frac{\lambda^2}{2\pi c d}\frac{d}{d\lambda}\mathrm{Im}(\ln(t_{1,2})) = = -\frac{\lambda^2}{2\pi c d}\mathrm{Im}\left(\frac{1}{t_{1,2}}\frac{dt_{1,2}}{d\lambda}\right), \quad (3)$$

where $t_{1,2}$ are the amplitudes of the transmitted wave, the values $m = 1, 2$ correspond to eigenmodes of the CLC layer, d is the CLC layer thickness, λ is the light wavelength. As in [33, 34], the effect of losses and gain we incorporate into analysis through introducing a small imaginary part to the dielectric constants parallel and perpendicular to the director: $\varepsilon_{1,2} = \mathrm{Re}\varepsilon_{1,2} + i\mathrm{Im}\varepsilon_{1,2}$, $\mathrm{Im}\varepsilon_{1,2} > 0$ corresponds to absorption case and $\mathrm{Im}\varepsilon_{1,2} < 0$, to amplifying case. And the director is the unit vector specifying the preferential orientation of the long axes of CLC molecules which uniformly rotates in the plane perpendicular to helix axis. Below we will investigate some new peculiarities of relative photonic density of states of CLC layer eigenmodes $PDS_{1,2} = \rho_{1,2}/\rho_{iso}$ spectra. Here $\rho_{iso} = \sqrt{\varepsilon_m}/c$.

We investigated also the peculiarities of spectra of the light energy density in the CLC layer at the isotropic and anisotropic absorption and gain cases, for two eigenmodes of CLC layer. The light energy density in the CLC layer will be calculated using the following formula [35]:

$$w = \frac{1}{d}\int_0^d \left|E_{in}(z)\right|^2 dz, \quad (4)$$

where $E_{in}(z)$ is total field in the CLC layer in the z point, and axis z directed along the CLC helix axis.

Now we pass to investigate the thresholds of laser generation at edge modes. First of all, in this paper we do not take into account nonlinear effects like pump depletion, so the amplification coefficient is uniform and fixed along the entire volume of the structure. However, since we consider the pre-threshold regime and moreover, a very thin longitudinally active region, the pump depletion can be neglected. Nevertheless, it can be assumed that a strict account of depletion will lead to a small increase in the threshold in the whole spectrum and a small change in the longitudinal gain distribution and field distribution, which in turn are determined by the specific pumping method.

We will consider our CLC to reach the lasing threshold when the transmission coefficients $t_{1,2}$ of the eigenmodes turn into infinity [36, 37]. This condition can be interpreted as when lasing is achieved, one can see a finite outcoming wave in the absence of any incoming wave. So, if the condition $1/t_{1,2}\left(\lambda, \mathrm{Im}\varepsilon_{1,2}\right)=0$ is satisfied for some pair of parameters $\left(\lambda_{th}, \mathrm{Im}\varepsilon_{th1,2}\right)$, where $\mathrm{Im}\varepsilon_{1,2}<0$ is the amplification, then the lasing is achieved at the wavelength λ_{th} with the lasing threshold $\mathrm{g}_{1,2}=\left|\mathrm{Im}\varepsilon_{th1,2}\right|$. It is also worth noting that the lasing can be achieved only at specific wavelengths while at all other wavelengths the lasing is impossible no matter how much the amplification is. These wavelengths are known as wavelengths of localized edge modes. Also, it's worth noting that in this paper we describe the amplification in terms of imaginary parts of dielectric permittivity components. Another common way to describe it is to use imaginary part of refractive indices but both methods can be used interchangeably.

In [38] an analytic theory of localized edge modes in CLCs was developed. The boundary value problem for localized eigen modes was solved for diffracting eigenpolarizations. To find these localized modes, they solve the homogeneous system of the above boundary value problem with zero values of E_{ir} and E_{il} amplitudes of the waves incident on the layer of CLC from the right and the left. The solvability condition of the obtained homogeneous system determines the discrete frequencies of these localized modes and has the following form [38]

$$\tan\left(Kd\right)=\frac{i\left(\dfrac{K\lambda^2}{\pi p\bar{\varepsilon}}\right)}{\chi^2+\left(\dfrac{K\lambda}{2\pi\sqrt{\bar{\varepsilon}}}\right)^2-1}, \tag{5}$$

where $K=(2\pi/\lambda)\sqrt{\bar{\varepsilon}}\sqrt{1+\chi^2-\gamma}$, is the resonant wave number of CLC determining from (2), $\gamma=\sqrt{4\chi^2+\delta^2}$, $\chi=\lambda/p\sqrt{\bar{\varepsilon}}$. In the general case, solutions of (4) for the edge mode frequencies ω_{EM} can only be found numerically. The edge mode frequencies ω_{EM} turn out to be complex quantities, which can be written $\omega_{EM}=\omega_0\left(1+i\Delta\right)$, where Δ is a small parameter in real situations. At sufficiently small Δ, ensuring the condition $\mathrm{Im}K\ll 1/d$ these wavelengths approximately coincide with the zeros of the reflection coefficient at absence of absorption, determined by the conditions [38]:

$$Kd=m\pi, \tag{6}$$

where m is the edge mode number, which increases as the wavelength departs from the PBG edge ($m=1$ corresponds to the wavelength closest to the PBG edge).

Two primary factors are important for band edge laser emission to occur in CLC structure [10]. First, an active medium of some form must be present. This can be either a rare-earth element or a laser dye. The dye can either be dispersed into the liquid-crystal matrix or it can form a subunit of the liquid-crystalline molecule. The second factor is the spectral position of the PBG relative to the emission spectrum of the light emitter. To achieve laser action, one of edges of the PBG or both must overlap the emission spectrum, and these must be matched to maximize coupling efficiency and thus achieve the lowest possible threshold. Then, we must keep in mind that the dye-doped CLC layer is an absorbing medium, and it becomes amplifying in the presence of pumping beam.

Now let us proceed with the study of the calculation of the laser generation thresholds and the peculiarities of light localization. We will calculate the exact values for the laser thresholds on the basis of the Berreman method [39], and the field in the CLC by the method described in [35, 40], without any approximations. Then we compare these exact values for laser generation thresholds with their approximate analytical expression for laser thresholds obtained in [38, 41, 42].

Fig. 2 shows the spectrum of PDS for diffracting eigenmode at the absence of absorption and gain (solid line) and values of threshold $\mathrm{g}=\left(\mathrm{g}_1+\mathrm{g}_2\right)/2$ for the same eigenmode in the case of isotropic and anisotropic gain. First of all, in Fig. 2 we can clearly see also the decrease in the lasing threshold of laser modes near the boundaries of the PBG, while inside the PBG itself laser generation is not observed at all. But it is interesting that this change does not take place continuously for all wavelengths, but in discrete paces, as mentioned above. It takes place only on edge modes wavelengths. Let us note also that unlike the PDS in a quarter-wave stack [43], the PDS profile of a non-absorbing CLC is nonsymmetric with respect to the center of the PBG. The shortwave peak of PDS turns out to be larger than the longwave one. And, as can be seen in Fig. 2 at isotropic gain the value of shortwave threshold for edge mode with $m=1$ is slightly smaller than the longwave one.

Interesting features are observed in cases of anisotropic amplification, in particular, there appears a pronounced asymmetry in the wavelength dependence of thresholds with respect to the center of the PBG. In the case of at $\mathrm{g}_1\neq 0$ and $\mathrm{g}_2=0$, the thresholds of laser generation on short-wavelength edge modes are much larger than on the corresponding modes in the case of isotropic gain. And on long-wavelength edge modes the thresholds decrease in comparison with the case of isotropic gain. In the case at $\mathrm{g}_1=0$ and $\mathrm{g}_2\neq 0$ we have the opposite picture. Let us pay special attention also to the fact that the threshold values for the first short-wave mode at $\mathrm{g}_1=0$ and $\mathrm{g}_2\neq 0$ and for the first long-wave mode at $\mathrm{g}_1\neq 0$ and $\mathrm{g}_2=0$ are less than the corresponding threshold values at isotropic gain. This is due to the effects of anomalously strong absorption/amplification and absorption/amplification suppression effects in CLC [34, 44]. As well-known if the incident light has the diffracting EP and if the light frequency is in the PBG region then the total wave exited in the medium has linear polarization. Then, if the frequency of light varies the angle between directions of an electrical field of a total wave and the CLC local director also vary and near the short-wavelength boundary of a PBG the total wave field appears directed along the direction perpendicular to local director (appropriate to direction ε_2). With the increase in the incident light wavelength the total-wave field direction rotates and near the long-wavelength boundary of a PBG the total wave field is directed along the local director (appropriate to direction ε_1). Therefore, when the oscillators of absorption in the molecules of CLC are directed along the director, then at the long-wavelength boundary of the PBG the anomalously weak absorption will be observed. When the oscillators of absorption are directed perpendicularly to the direction of the director, minimum absorption will be observed at the short-wavelength boundary of the diffraction reflection region. Outside the PBG, this total wave has an elliptical polarization with the lowest ellipticity near the boundaries of the PBG. As we move away from the PBG, the ellipticity of this total wave increases and away from the PBG the total wave has almost circular polarization.

Let us note that for the majority of the studies carried out so far, the long-wavelength band edge has proven to be the lowest-threshold mode. It is because the transient dipole moment of the dye is usually spontaneously orientated along with the local director at each point, which corresponds to the case $g_1 \neq 0$ and $g_2 = 0$, and that the long wavelength part of PBG usually overlap the emission spectrum in these experiments and, moreover total wave field appears directed along this direction. Let us also note here that the isotropic gain $g_2 = g_1 \neq 0$ case corresponds to an isotropic orientational distribution of the transition dipole moments to the local director.

Thus, in order to experimentally detect a significant difference between the thresholds near the two PBG boundaries in the two cases of anisotropic gain, in particular, to detect that the lowest threshold must observed on the first shortwave edge mode, it is necessary to perform laser generation experiments with the same CLC with the addition of dyes in it of two types, namely with a dye whose transition dipole moment of dye molecules spontaneously orientate along the local director of the CLC at any point of the structure and secondly with a dye whose transition dipole moment of dye molecules spontaneously orientate perpendicular to the local director of the CLC at any point of the structure. As already mentioned, experiments of the first type have already been carried out. To obtain dyes the transient dipole moment of molecules which can spontaneously orientate in a certain direction relative to the director and the dye molecules orientation mechanisms is of great interest and research in this direction is being carried out intensively [45 – 47].

Of cause, for the dye emission (as well as for the pumping beam propagation inside the active medium), in real experimental situations one has to take into account various loss mechanisms too, including linear absorption, light scattering from imperfections, cavity losses due to light escaping from the cavity, and Förster resonance energy transfer when two chromophores are involved [10].

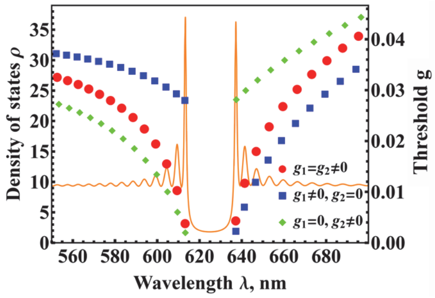

Fig. 2. The spectrum of PDS for diffracting EP at the absence of absorption and gain (solid line) and values of threshold g for lasing modes in the isotropic (red dots: $g_1 = g_2 \neq 0$ and anisotropic (blue dots: $g_1 \neq 0, g_2 = 0$; green dots: $g_1 = 0,\ g_2 \neq 0$) gain cases

Now we investigate the peculiarities of the light field intensity $|E_{in}|^2$ distribution inside the CLC layer at the presence of gain and the energy density w spectra peculiarities of CLC layer at the presence of absorption and gain. As shown in [34, 37] usually $w \propto PDS$, and $|E_{in}(z)|^2$ at the absence of absorption and gain shows the local PDS.

Fig. 3 shows the dependence of $|E_{in}(z)|^2$ at the absence of absorption and gain (curve 1) and at the presence of gain (curves 2 and 3). As it is seen on Fig.3 the presence of gain (of course at its small values, see below) brings to increase in $|E_{in}|^2$ and with increase of gain the change of wavelength of edge modes take place, too (at $\mathrm{Im}\varepsilon_1 = \mathrm{Im}\varepsilon_2 = 0$ and at $\mathrm{Im}\varepsilon_1 = \mathrm{Im}\varepsilon_2 = -10^{-4}$ for edge mode $n = 1$ we have $\lambda = 613.1$ nm, while at $\mathrm{Im}\varepsilon_1 = \mathrm{Im}\varepsilon_2 = -10^{-3}$ we have $\lambda = 613.3$ nm).

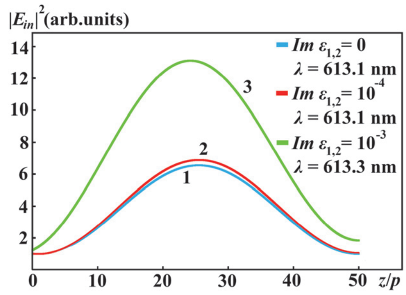

Fig. 3. The dependence of $|E_{in}(z)|^2$ at the absence of absorption and gain (curve 1) and at the presence of gain at (curves 2 and 3) on the first short wavelength edge mode with $n = 1$. 1: $\mathrm{Im}\varepsilon_1 = \mathrm{Im}\varepsilon_2 = 0; \lambda = 613.1\,nm$. 2: $\mathrm{Im}\varepsilon_1 = \mathrm{Im}\varepsilon_2 = -10^{-4}; \lambda = 613.1\,nm$. 3: $\mathrm{Im}\varepsilon_1 = \mathrm{Im}\varepsilon_2 = -10^{-3}; \lambda = 613.3\,nm$

Fig. 4 shows the evolution of the energy density w spectra for the case when the absorption (left column) and gain (right column) increases. Absorption and amplification we characterize by the parameter $x = \ln(|\mathrm{Im}\varepsilon_m|)$. The first row corresponds to the isotropic absorption and gain ($\mathrm{Im}\varepsilon_1 = \mathrm{Im}\varepsilon_2$), the second row corresponds to the anisotropic absorption/gain case with $\mathrm{Im}\varepsilon_1 \neq 0, \mathrm{Im}\varepsilon_2 = 0$, and finally, the third row is for the case of the anisotropic absorption/gain case with $\mathrm{Im}\varepsilon_1 = 0, \mathrm{Im}\varepsilon_2 \neq 0$.

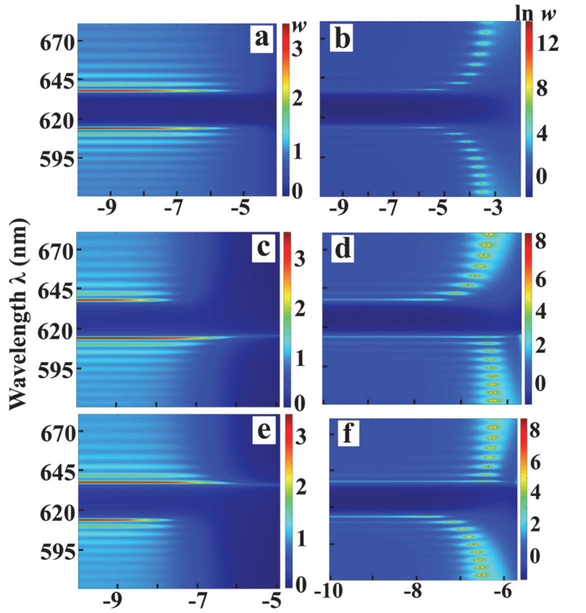

Fig. 4. The evolution of the energy density w spectra for the case when the absorption (left column) and gain (right column) increase. Absorption and gain is characterized by the parameter $x = \ln(|\mathrm{Im}\varepsilon_m|)$. The first row corresponds to the isotropic absorption and gain ($\mathrm{Im}\varepsilon_1 = \mathrm{Im}\varepsilon_2$), the second row corresponds to the anisotropic absorption/gain case with $\mathrm{Im}\varepsilon_1 \neq 0, \mathrm{Im}\varepsilon_2 = 0$, and finally, the third row is for the case of the anisotropic absorption/gain case with $\mathrm{Im}\varepsilon_1 = 0, \mathrm{Im}\varepsilon_2 \neq 0$

When the absorption increases, the w on edge modes monotonically decreases. While, when the gain increases, the w is increased too, however the further increment of the gain leads to a resonance-like change in the w and then the w is diminished. There is a critical value of the parameter x beyond which the localisation of light resonantly decreases. Note that the critical values of x for the short wavelength edge modes and long wavelength edge modes with the same *m* are different. At anisotropic absorption/gain there appears asymmetry, which is due to the mentioned effects of anomalously strong absorption/amplification and absorption/amplification suppression effects in CLC.

As well known (see [41]) for weak absorption (gain) and small *d*Im*K* the reflection and transmission coefficients for CLC layer approximately are defined by the following expressions for the edge modes:

$$R = \frac{(a^3\gamma)^2}{\left((\pi m)^2 + a^3\gamma\right)^2}, \quad T = \frac{(\pi m)^4}{\left((\pi m)^2 + a^3\gamma\right)^2}, \tag{7}$$

where $a = \pi\delta d/p$, $\gamma = \mathrm{Im}\bar{\varepsilon}/\delta\,\mathrm{Re}\,\bar{\varepsilon}$. In the case of amplification, γ is negative and, consequently, if:

$$\gamma = -\frac{(m\pi)^2}{a^3} = -\left((m\pi)^2 \Big/ \left(\frac{\pi\delta d}{p}\right)^3\right), \tag{8}$$

then the reflection and transmission coefficients diverge. As shown in [1], if the imaginary part of the dielectric tensor is negative and increases in absolute value, the value of $R+T$ becomes greater than unity, which corresponds to the amplifying medium. And when this value reaches some critical negative value, the values of R and T diverge and the amplitudes of waves leaving the layer become non-zero even at zero amplitudes of incident waves. Therefore, the value γ determined by expression (8) can be interpreted as the threshold value of laser generation, i.e. in this case we will have $\mathrm{g} = \gamma\delta\mathrm{Re}\varepsilon_m$.

And now the question arises how well formula (8) describes the generation threshold in general.

As is seen from (8), the minimum threshold value of $|\gamma|$ corresponds to the mode with $m = 1$, i.e. to the mode nearest to the PBG laser mode, and the threshold value of γ increases if m is increased. The same results were obtained by us numerically, presented in Fig. 2.

Fig.5 shows the comparison of thresholds for different edge mode numbers calculated numerically from the condition $1/T \to 0$ and analytically in accordance with equation $\mathrm{g} = \gamma\delta\mathrm{Re}\varepsilon_m$ with $\gamma = -\left((m\pi)^2 / (\pi\delta d/p)^3\right)$. The comparison demonstrates that the smaller edge number m is, the closer the analytically found and numerically calculated threshold gains are. This fact is in good agreement with the spectral dependence of *d*Im*K* value where only for the closest to PBG modes the condition Im*K*<<1/d is somewhat satisfied, and the analytical formula is accurate.

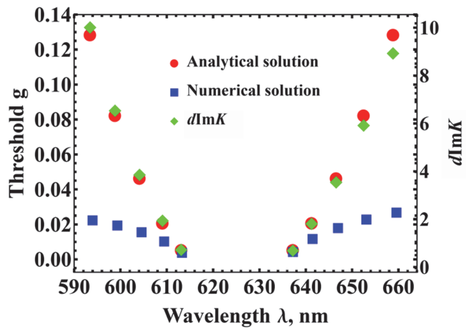

Fig. 5. Comparison of thresholds for different edge mode numbers calculated numerically from the condition 1/T→0 and analytically in accordance with equation $\mathrm{g} = \gamma\delta\mathrm{Re}\varepsilon_m$

Fig.6 shows the comparison of thresholds for different CLC layer thicknesses in the case of isotropic and anisotropic gain, for short wavelength (left) and long wavelength (right) edge modes with *m*=1 and *m*=2 numbers calculated numerically from the condition $1/T \to 0$ and analytically in accordance with equation $\mathrm{g} = \gamma\delta\mathrm{Re}\varepsilon_m$ with $\gamma = -\left((m\pi)^2 / (\pi\delta d/p)^3\right)$. The comparison demonstrates that the thicker CLC layer is, the closer the analytically found and numerically calculated threshold gains are.

Let us note that, in practice, the lasing threshold usually decreases with an increase of a CLC layer thickness only up to a certain value and then gradually increases slightly [20]. The last one is due to the longitudinal optical pumping (approximately along the helix axis), when gradual absorption of the pumping energy across the layer thickness results in decreasing the gain of the medium. While, as shown above (see also [1,38,41,42]), in the case of homogeneous gain distribution the lasing threshold gain decreases as a cube of the distributed feedback length.

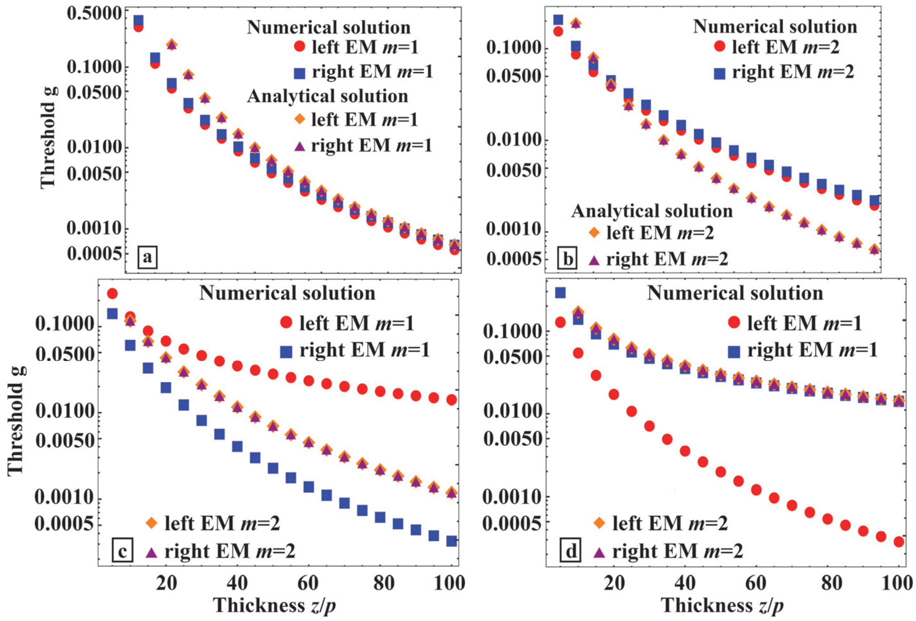

Fig. 6. The comparison of thresholds for different CLC layer thicknesses in the case of isotropic and anisotropic gain, for short wavelength (left) and long wavelength (right) edge modes with m=1 and m=2 numbers calculated numerically from the condition $1/T \to 0$ *and analytically in accordance with equation* $g = \gamma\delta Re\varepsilon_m$ *with* $\gamma = -\left((m\pi)^2 / (\pi\delta d/p)^3\right)$. *a, b)* $\mathrm{Im}\varepsilon_1 = \mathrm{Im}\varepsilon_2$, *c)* $\mathrm{Im}\varepsilon_1 \neq 0, \mathrm{Im}\varepsilon_2 = 0$, *d)* $\mathrm{Im}\varepsilon_1 = 0, \mathrm{Im}\varepsilon_2 \neq 0$

Conclusion

In conclusion, the laser threshold of the EPs on edge modes in CLC cells are calculated. The influence of gain on light localization was investigated, too. The influence of absorption and gain on the light energy density in the CLC layer both at isotropic and anisotropic absorption and gain were investigated. The calculated threshold values compared with analytical expression for laser threshold obtained in the condition ImK<<1/d.

As mentioned in the introduction the CLC layer gives rise to a polarization-sensitive laser generation. The generated low threshold laser light has polarization coinciding with the polarization of diffracting EP, that is unlike in isotropic PCs it has circular polarization. In general EPs of CLC depend on the local anisotropy of CLC and on n_s too. And this polarization can be continuously changed from circular to linear by appropriate changes of these parameters [48, 49].

Let us note once more that the subject problem on transmittance of radiation through a planar resonator with an active element and a constant amplification coefficient is not adequate to a real process. The amplification coefficient decreases as the intensity of the propagating through the medium wave increases. This is connected with the peculiarities of appearing of the inverse state – at very large energies accumulated in the laser active element, the speed of stimulated transitions prevails over the pumping speed. This leads to a sharp decrease in the difference of population of exited and ground states, which, in its turn, leads to a decrease in the amplification coefficient and, consequently, to the saturation of intensity [50]. And, as the interaction of radiation with the amplifying medium becomes neither linear, nor stationary, the linear approximation cannot be applied to the subject problem. Nevertheless, the presented results give much information on radiation peculiarities and laser generation in the CLC.

Acknowledgements

For AHG and AVB the work was carried out within the framework of the state projects: reg. No. 124042300003-5.

Conflict of interest

No potential conflict of interest was reported by the authors.

References

[1] Kogelnik H, Shank CV. Coupled-wave theory of distributed feedback lasers. J Appl Phys 1972; 43(5): 2327-2335. DOI: 10.1063/1.1661499.
[2] Yariv A, Nakamura M. Periodic structures for integrated optics. IEEE J Quantum Electron 1977; 13(4): 233-253. DOI: 10.1109/JQE.1977.1069323.
[3] Dowling JP, Scalora M, Bloemer MJ, et al. The photonic band edge laser: A new approach to gain enhancement. J Appl Phys 1994; 75(4): 1896-1899. DOI: 10.1063/1.356336.
[4] Kopp VI, Fan B, Vithana HKM, et al. Low-threshold lasing at the edge of a photonic stop band in cholesteric liquid crystals. Opt Lett 1998; 23(21): 1707-1709. DOI: 10.1364/OL.23.001707.

[5] Taheri B, Munoz A, Palffy-Muhoray P, et al. Low threshold lasing in cholesteric liquid crystals. Mol Cryst Liq Cryst Sci Technol. Sect A. Mol Cryst Liq Cryst 2001; 358(1): 73-82. DOI: 10.1080/10587250108028271.
[6] Il'chishin I, Tikhonov E, Tishchenko V, Shpak M. Generation of a tunable radiation by impurity cholesteric liquid crystals. J Exp Theor Phys Lett 1980; 32(1): 24-27.
[7] Blinov LM, Cipparrone G, et al. Mirrorless lasing from nematic liquid crystals in the plane waveguide geometry without refractive index or gain modulation. Appl Phys Lett 2006; 89(3): 0311114. DOI: 10.1063/1.2234316.
[8] Palto SP, Shtykov NM, et al. General properties of lasing effect in chiral liquid crystals. Opto Electron Rev 2006; 14: 323. DOI: 10.2478/s11772-006-0044-7.
[9] Shtykov NM, Palto SP. Modeling laser generation in cholesteric liquid crystals using kinetic equations. J Exp Theor Phys 2014; 118(5): 822-830. DOI: 10.1134/S1063776114040074.
[10] Coles H, Morris S. Liquid-crystal lasers. Nat Photonics 2010; 4(10): 676-685. DOI: 10.1038/nphoton.2010.184.
[11] Gao S, Wang J, Li W, et al. Low threshold random lasing in dye-doped and strongly disordered chiral liquid crystals. Photonics Res 2020; 8(5): 642-647. DOI: 10.1364/PRJ.388706.
[12] Blinov LM, Bartolino R. Liquid crystal microlasers. Kerala: Transworld Research Network; 2010.
[13] Mysliwiec J, Szukalska A, Szukalski A, et al. Liquid crystal lasers: the last decade and the future. Nanophotonics 2021; 10(9): 2309-2346. DOI: 10.1515/nanoph-2021-0096.
[14] Zaplotnik J, Mur U, Malkar D, et al. Photonic eigenmodes and transmittance of finite-length 1D cholesteric liquid crystal resonators. Sci Rep 2023; 13(1): 16868. DOI: 10.1038/s41598-023-43912-2.
[15] Lin JH, Shih WC, Xie ZH, et al. Thermal control band-edge lasing toward near IR from dye-doped cholesteric liquid crystal: Relatively stable operation at high temperatures. Opt Laser Technol 2024; 174: 110592. DOI: 10.1016/j.optlastec.2024.110592.
[16] Wang Y, Manabe T, Takanishi Y, et al. Dependence of lasing threshold power on excitation wavelength in dye-doped cholesteric liquid crystals. Opt Commun 2007; 280(2): 408-411. DOI: 10.1016/j.optcom.2007.08.027.
[17] Blinov LM. Lasers on cholesteric liquid crystals: Mode density and lasing threshold. JETP Lett 2009; 90: 166-171. DOI: 10.1134/S0021364009150028.
[18] Shtykov NM, Palto SP, Geivandov AR, et al. Lasing in liquid crystal systems with a deformed lying helix. Opt Lett 2020; 45(15): 4328-4331. DOI: 10.1364/OL.394430.
[19] Porov P, Chandel VS, Manohar R. Lasing characteristics of dye-doped cholesteric liquid crystal. Trans Electr Electron Mater 2015; 16(3): 117-123. DOI: 10.4313/TEEM.2015.16.3.117.
[20] Cao W, Palffy-Muhoray P, Taheri B, et al. Lasing thresholds of cholesteric liquid crystals lasers. Mol Cryst Liq Cryst 2005; 429(1): 101-110. DOI: 10.1080/15421400590930782.
[21] Folcia CL, Ortega J, Sierra T, et al. Chiral ferroelectric nematic liquid crystals as materials for versatile laser devices. Giant 2024; 19: 100316. DOI: 10.1016/j.giant.2024.100316.
[22] Lu H, Wei C, Zhang Q, et al. Wide tunable laser based on electrically regulated bandwidth broadening in polymer-stabilized cholesteric liquid crystal. Photonics Res 2019; 7(2): 137-143. DOI: 10.1364/PRJ.7.000137.
[23] Lin JD, Lin HL, Lin HY, et al. Widely tunable photonic bandgap and lasing emission in enantiomorphic cholesteric liquid crystal templates. J Mater Chem C 2017; 5(13): 3222-3228. DOI: 10.1039/C7TC00090A.
[24] Lin JD, Lin HY, Wei GJ, et al. A broadband-tunable photonic bandgap and thermally convertible laser with an ultra-low lasing threshold from a refilled chiral polymer template. J Mater Chem C 2019; 7(16): 4740-4747. DOI: 10.1039/C9TC00194H.
[25] Shtykov NM, Palto SP, et al. Lasing in a nematic liquid crystal cell with an interdigitated electrode system. Quantum Electron 2015; 45(4): 305. DOI: 10.1070/QE2015v045n04ABEH015717.
[26] Shtykov NM, Palto SP, et al. Fluorescence and lasing in an electric-field-induced periodic structure of a cholesteric liquid crystal. Quantum Electron 2019; 49(8): 754-761. DOI: 10.1070/QEL16898.
[27] Moreira MF, Relaix S, Cao W, et al. Liquid crystal microlasers. Kerala, India: Transworld Research Network; 2010.
[28] Dolgaleva K, Wei SKH, Lukishova SG, et al. Enhanced laser performance of cholesteric liquid crystals doped with oligofluorene dye. J Opt Soc Am B 2008; 25(9): 496-1504. DOI: 10.1364/JOSAB.25.001496.
[29] De Vries HL. Rotatory power and other optical properties of certain liquid crystals. Acta Cryst 1951; 4: 219-226. DOI: 10.1107/S0365110X51000751.
[30] Kats EI. Optical properties of cholesteric liquid crystals. JETP 1971; 32(5): 1004-1007.
[31] Gevorgyan AA. Reflection and transmission of light for a layer with dielectric and magnetic helicities. I. Jones matrices. Natural polarizations. Opt Spectrosc 2000; 89(4): 631-638. DOI: 10.1134/BF03356031.
[32] D'Aguanno G, Mattiucci N, Scalora M, Bloemer MJ, Zheltikov AM. Density of modes and tunneling times in finite one-dimensional photonic crystals: a comprehensive analysis. Phys Rev 2004; 70(1): 016612. DOI: 10.1103/PhysRevE.70.016612.
[33] Mavrogordantos TK, Morris S, Castles F, et al. Density of photon states in dye-doped chiral nematic liquid crystal cells in the presence of losses and gain. Phys Rev E 2012; 86(1): 011705. DOI: 10.1103/PhysRevE.86.011705.
[34] Gevorgyan AH, Oganesyan KB, Vardanyan GA, et al. Photonic density of states of cholesteric liquid crystal cells. Laser Phys 2014; 24(11): 115801. DOI: 10.1088/1054-660X/24/11/115801.
[35] Gevorgyan AH. Broadband optical diode and giant nonreciprocal tunable light localization. Opt Mater 2021; 113: 110807. DOI: 10.1016/j.optmat.2021.110807.
[36] Yariv A, Yeh P. Optical waves in crystals. New York: Wiley; 1984.
[37] Vanyushkin NA, Gevorgyan AH. And again, about lasing threshold, light localization, and density of states in 1D photonic crystals. Photonics Nanostructures – Fundam Appl 2023; 54: 101134. DOI: 10.1016/j.photonics.2023.101134.
[38] Belyakov VA, Semenov SV. Optical edge modes in photonic liquid crystals. JETP 2009; 109: 687-699. DOI: 10.1134/S106377610910015X.
[39] Berreman DW. Optics in stratified and anisotropic media: 4x4-matrix formulation. J Opt Soc Am 1972; 62(4): 502-510. DOI: 10.1364/JOSA.62.000502.
[40] Gevorgyan AH. Light absorption suppression in cholesteric liquid crystals with magneto-optical activity. J Mol Liq 2021; 335: 116-289. DOI: 10.1016/j.molliq.2021.116289.
[41] Belyakov VA, Gevorgian AA, Eritsian OS, Shipov NV. Anomalous absorption of radiation in periodic media near the boundaries of forbidden-propagation bands. Sov Phys Tech Phys 1987; 32(7): 843-845.

[42] Gevorgyan AH, Oganesyan KB, Harutyunyan EM, Arutyunyan SO. The peculiarities of radiation of chiral photonic crystals with isotropic defect layer. Opt Commun 2010; 283: 3707-3713. DOI: 10.1016/j.optcom.2010.05.044.
[43] Bendickson JM, Dowling JP, Scalora M. Analytic expressions for the electromagnetic mode density in finite, one-dimensional, photonic band-gap structures. Phys Rev E 1996; 53(4): 4107. DOI: 10.1103/PhysRevE.53.4107.
[44] Gevorgyan AH. Mechanisms of anomalous absorption of radiation in media with periodical structure. Mol Cryst Liq Cryst 2002; 378(1): 129-146. DOI: 10.1080/713738580.
[45] Friederich P, Coehoorn R, Wenzel W. Molecular origin of the anisotropic dye orientation in emissive layers of organic light emitting diodes. Chem Mater 2017; 29(21): 9528-9535. DOI: 10.1021/acs.chemmater.7b03742.
[46] Ohzono T, Yatabe T, Wang C, et al. Negative fluorescence anisotropy of phosphole oxide-based dyes in nematic liquid crystals. Commun Chem 2018; 1(1): 52. DOI: 10.1038/s42004-018-0055-6.
[47] Nguyen M, Schmid M, Kirsch J, et al. On the orientation mechanism of nonpolar dyes in light-emitting guest–host systems. Chem Mater 2023; 35(17): 7333-7343. DOI: 10.1021/acs.chemmater.3c01804.
[48] Gevorgyan AA. Reflection and transmission of light in medium /cholesteric/ substrate and glass (1) / cholesteric / glass (2) systems. Tech Phys 2000; 45(9): 1170-1176. DOI: 10.1134/1.1318104.
[49] Gevorgyan AH, Harutyunyan MZ, Kocharian A, Vardanyan GA. Selective diffraction reflection in helical periodical media with large anisotropy. Mol Cryst Liq Cryst 2005; 432: 69-83. DOI: 10.1080/154214090960153.
[50] Svelto O. Principles of lasers. New York: Plenum; 1982. ISBN: 0-3064-0862-7.

Authors' information

Andrey Alexandrovich Malinchenko (b. 2001) received a bachelor's degree in chemical engineering from Far Eastern Federal University in 2023. Currently he is a second-year master student in the direction of "applied physics" at FEFU. He has authored and co-authored more than 7 papers that have been published at conferences and in journals.
E-mail: *malinchenko.aal@dvfu.ru*

Nikolay Aleksandrovich Vanyushkin (b. 1995) received the bachelor's and the master's degree in applied mathematics and physics from the Moscow Institute of Physics and Technology, Moscow, Russia, in 2018 and 2020, respectively. He was with NTO IRE-Polus, Fryazino, Russia, as a research intern from 2017 to 2020. He joined the Far Eastern Federal University, Vladivostok, Russia, where he has been working as a research engineer from 2021 to 2022. He has authored and co-authored over 30 conference and journal refereed papers. E-mail: *vaniuschkin.nick@ya.ru*

Alexey Vladimirovich Bulanov (b. 1985) received the Ph.D. degree in «laser physics» in 2009. He is the author of more than 30 scientific papers in peer-reviewed journals indexed in Scopus/Web of Science (the total number of his scientific and educational works is more than 60. He has rich experience in scientific activities: he worked for 20 years as a young researcher, researcher, senior researcher in Pacific Oceanological Institute Far Eastern Branch of the Russian Academy of Science. Now he is the head of laboratory in POI FEB RAS. E-mail: *a_bulanov@poi.dvo.ru*

Ashot Harutyunovich Gevorgyan (b. 1958) received the Ph.D. degree in physics from Institute of Applied Problems in Physics, Yerevan, Armenia, in 1987 and Doctor of Science in 2010. He is the author of more than 200 scientific papers in peer-reviewed journals indexed in Scopus/Web of Science (the total number of his scientific and educational works is more than 345. He also has a rich experience in educational activities: he worked for 37 years as an assistant and associate professor in the department of general physics at Yerevan State University, since 2010 as a professor of the department, and in 2018-2019 he headed this department. He joined the Far Eastern Federal University, Vladivostok, Russia, in 2019, where he is currently a professor. E-mail: *agevorgyan@ysu.am*

Received November 17, 2024. The final version – March 16, 2025.